DOE/ET-53088-410 IFSR #410

Point Vortex Description of Drift Wave Vortices: Dynamics and Transport

M. KONO
Research Institute for Applied Mechanics, Kyushu University,
Kasuga, Fukuoka, 816, Japan
and
W. HORTON
Institute for Fusion Studies
The University of Texas at Austin
Austin, Texas 78712

May 1991

REVISED

Point Vortex Description of Drift Wave Vortices: Dynamics and Transport

M. Kono[a] and W. Horton
Institute for Fusion Studies
The University of Texas at Austin
Austin, Texas 78712

Abstract

Point vortex description for drift wave vortices is formulated based on the Hasegawa-Mima equation to study elementary processes for the interactions of vortices as well as statistical properties like vortex diffusion. Dynamical properties of drift wave vortices known by numerical experiments are recovered. Furthermore a vortex diffusion model discussed by Horton [Phys. Fluids **31**, 326 (1989)] based on numerical simulations is shown to be analytically obtained. A variety of phenomena arising from the short-range nature of the interaction force of point vortices are suggested.

[a] On leave from Research Institute for Applied Mechanics, Kyushu University, Kasuga, Fukuoka, 816, Japan

I. Introduction

Excitation and dynamics of drift wave vortices have been intensively studied in connection with the anomalous plasma transport since these coherent vortices are able to carry particles over long distances. Interactions of vortices, therefore are of central importance to obtain a full understanding of transport. Studies on dynamics of drift wave vortices have mainly been performed numerically based on the Hasegawa-Mima equation,[1] which is difficult to solve analytically. In this brief communication we derive point vortex equations of motion for the vortex cores in the point vortex limit from the Hasegawa-Mima equation and study elementary processes of interaction of the vortices, through the new dynamical equations. The dynamical equations for the interacting vortex cores provide a clear understanding of the dynamical properties of drift wave vortices as well as statistical properties of the associated plasma transport.

An advantage of introducing point vortices is to convert a nonlinear partial differential equation into a system of ordinary differential equations which easier to solve, while wave phenomena are neglected. A crucial difference of the Hasegawa-Mima equation from Euler's equation is the existence of the drift term giving rise to dispersive waves, which requires that the vorticity attached to each point vortex is no longer constant but varies in space and time, in contrast with the point vortex description of Euler's equation characterized by constant strength vorticities. This modulated point vortex model was first introduced by Kono-Yamagata[2] based on the fact that the Hasegawa-Mima equation conserves the vorticity along the trajectory, then later by Zabusky-McWilliams[3] who studied the configurations of the vortices corresponding to a stationary solution of the Hasegawa-Mima equation and stability of the configurations. In §2 we re-derive the point-vortex equation for the Hasegawa-Mima equation. In §3 an exact solution for a vortex-pair is obtained and is shown to recover the dynamical properties of the drift wave vortices revealed by numerical simulations. In §4

collision processes of two vortex-pairs are studied. In §5 a statistical theory of a many-vortex system is formulated where the vortex diffusion coefficient is analytically derived to give the empirical formula given by Horton.[4] Discussions are given in the last section.

II. Point Vortex Model

Starting with the Hasegawa-Mima equation

$$\frac{\partial \pi}{\partial t} + [\psi, \pi] + v_* \frac{\partial \psi}{\partial y} = 0 \ , \tag{1}$$

where [,] denotes the Poisson bracket and

$$\pi = \psi - \nabla^2 \psi \ , \tag{2}$$

we introduce the vortices through

$$\pi(\mathbf{r}, t) = \sum_\alpha \kappa_\alpha(t) V_\alpha(\mathbf{r} - \mathbf{r}_\alpha(t)) \ , \tag{3}$$

where $V_\alpha(\mathbf{r} - \mathbf{r}_\alpha(t))$ is a localized function at $\mathbf{r} = \mathbf{r}_\alpha(t)$ and $\mathbf{r}_\alpha(t)$ is determined by the characteristics of Eq. (1):

$$\frac{d\mathbf{r}_\alpha(t)}{dt} - [\psi(\mathbf{r}_\alpha, t), \mathbf{r}_\alpha] = 0 \ . \tag{4}$$

Substituting Eq. (3) into Eq. (1), we obtain

$$\sum_\alpha \frac{d\kappa_\alpha(t)}{dt} V_\alpha(\mathbf{r} - \mathbf{r}_\alpha) - \sum_\alpha \frac{\partial}{\partial \mathbf{r}} \cdot \left\{ \frac{d\mathbf{r}_\alpha}{dt} - \mathbf{z} \times \frac{\partial \psi(\mathbf{r}, t)}{\partial \mathbf{r}} \right\} V_\alpha(\mathbf{r} - \mathbf{r}_\alpha)$$

$$= -v_* \frac{\partial}{\partial y} \psi(\mathbf{r}, t) \ . \tag{5}$$

Since $V_\alpha(\mathbf{r} - \mathbf{r}_\alpha(t))$ is a function localized around $\mathbf{r} = \mathbf{r}_\alpha(t)$, we may replace the arguments $\mathbf{r}$ appeared in the coefficients of $V_\alpha(\mathbf{r} - \mathbf{r}_\alpha(t))$ by $\mathbf{r}_\alpha(t)$, and then the second term of the left-hand side of Eq. (5) vanishes according to Eq. (4). Then we have

$$\sum_\alpha = \frac{d\kappa_\alpha(t)}{dt} V_\alpha(\mathbf{r} - \mathbf{r}_\alpha) = -v_b s \frac{\partial}{\partial y} \psi(\mathbf{r}, t) \ . \tag{6}$$

Multiplying the both sides of Eq. (6) by $V_\beta(\mathbf{r}-\mathbf{r}_\beta)$ and integrating with respect to $\mathbf{r}$ where we may approximate the overlap integral as follows

$$\int d\mathbf{r} V_\alpha(\mathbf{r}-\mathbf{r}_\alpha(t))V_\beta(\mathbf{r}-\mathbf{r}_\beta(t)) \simeq \delta_{\alpha\beta} \ , \tag{7}$$

then we obtain

$$\frac{d\kappa_\alpha}{dt} = v_* \frac{dx_\alpha}{dt} \ . \tag{8}$$

When the localized function $V_\alpha(\mathbf{r}-\mathbf{r}_\alpha)$ is approximated by a delta function $\delta(\mathbf{r}-\mathbf{r}_\alpha)$, that is, the vortex is assumed a point vortex, we have from Eqs. (2) and (3)

$$\psi(\mathbf{r},t) = \frac{1}{2\pi}\sum_\alpha \kappa_\alpha(t) K_0(|\mathbf{r}-\mathbf{r}_\alpha|) \ , \tag{9}$$

where K_0 is the modified Bessel function of the first kind.

In the following we assume v_* positive and constant:

$$\kappa_\alpha(t) = \kappa_{\alpha 0} + v_* x_\alpha(t) \ , \tag{10}$$

where $\kappa_{\alpha 0}$ is a constant. Then Eq. (4) becomes

$$\frac{d\mathbf{r}_\alpha}{dt} = \frac{1}{2\pi}\sum_{\beta\neq\alpha}(\kappa_{\beta 0} + v_* x_\beta)\mathbf{z}\times\frac{\partial}{\partial \mathbf{r}_\alpha}K_0(r_{\alpha\beta}) \ , \tag{11}$$

where $r_{\alpha\beta} = |\mathbf{r}_\alpha(t) - \mathbf{r}_\beta(t)|$. Equation (11) has the same form as that introduced by Kono-Yamagata[2] first and then later by Zabusky-McWilliams[3] who introduced the name modulated point vortex for the variation $\kappa_\alpha = \kappa_{\alpha 0} + v_* x_\alpha$. The simple case of constant κ_α valid when $v_* = 0$ is studied by Hasegawa*et al.*[5]

There are two constants of motion for the Hasegawa-Mima equation; one is the energy

$$E = \frac{1}{2}\int d\mathbf{r}\left[\psi^2 + (\nabla\psi)^2\right] = \frac{1}{2}\int d\mathbf{r}\psi\pi \ , \tag{12}$$

and the other is the enstrophy

$$W = \frac{1}{2}\int d\mathbf{r}\left[(\nabla\psi)^2 + (\nabla^2\psi)^2\right] = -\frac{1}{2}\int d\mathbf{r}(\nabla^2\psi)\pi \ . \tag{13}$$

In the point vortex description the energy and enstrophy are expressed as

$$E = \frac{1}{2\pi}\sum_{\alpha\neq\beta}(\kappa_{\alpha 0} + v_* x_\alpha)(\kappa_{\beta 0} + v_* x_\beta)K_0(r_{\alpha\beta}) \ , \tag{14}$$

$$W = \frac{1}{4\pi}\sum_{\alpha\neq\beta}(\kappa_{\alpha 0} + v_* x_\alpha)(\kappa_{\beta 0} + v_* x_\beta)[K_0(r_{\alpha\beta}) + K_2(r_{\alpha\beta})] \ , \tag{15}$$

where the self-energy has been subtracted since it diverges. Equation (14) is not a Hamiltonian of the dynamical system of the vortices. Instead the Hamiltonian is given by

$$H = \sum_\alpha \psi(\mathbf{r}_\alpha) \ , \tag{16}$$

from which we have

$$\frac{dx_\alpha}{dt} = -\frac{\partial H}{\partial y_\alpha} = \frac{1}{2\pi}\sum_\beta(\kappa_{\beta 0} + v_* x_\beta)\frac{y_\alpha - y_\beta}{r_{\alpha\beta}}K_1(r_{\alpha\beta}) \ , \tag{17}$$

$$\frac{dy_\alpha}{dt} = \frac{\partial H}{\partial x_\alpha} = -\frac{1}{2\pi}\sum_\beta(\kappa_{\beta 0} + v_* x_\beta)\frac{x_\alpha - x_\beta}{r_{\alpha\beta}}K_1(r_{\alpha\beta}) \ . \tag{18}$$

Since H is translationally invariant along the y-axis, the translational momentum in x is conserved:

$$P = \sum_\alpha(\kappa_{\alpha 0} + v_* x_\alpha)^2 \ . \tag{19}$$

III. Vortex-Pair Solution

Now we slove Eqs. (17) and (18) for two vortices. In this case in addition to Eq. (19) the relative distance of the vortices is a constant of motion.

$$r_{12}^2 = (x_1 - x_2)^2 + y_1 - y_2)^2 = r_0^2 \ , \tag{20}$$

which leads to

$$\frac{d}{dt}\cos\theta = \pm\frac{v_* K_1(r_0)}{2\pi}\sqrt{(A + \cos\theta)(B - cos\theta)(1 - \cos^2\theta)} \ , \tag{21}$$

where $x_1 - x_2 = r_0 \cos\theta$, $A = \left[\sqrt{2P} + (\kappa_{10} - \kappa_{10})\right] / v_* r_0$, and $B = \left[\sqrt{2P} - (\kappa_{10} - \kappa_{20})\right] / v_* r_0$. Equation (20) is readily integrated to yield a solution expressed in terms of the Jacobi elliptic function. The solution is given by

$$\cos\theta = \gamma \frac{1 - \beta^2 sn^2(\omega t, k)}{1 - \alpha^2 sn^2(\omega t, k)} , \tag{22}$$

where for $v_* r_0 + |\kappa_{10} - \kappa_{20}| > \sqrt{2P} > |v_* r_0 - |\kappa_{10} - \kappa_{20}||$

$$\alpha^2 = \frac{1+B}{A+B}, \quad \beta^2 = A\alpha^2, \quad \gamma = -\mathrm{sgn}(\kappa_{10} - \kappa_{20}) \tag{23}$$

$$\omega = \sqrt{2(A+B)} \frac{v_* K_1(r_o)}{4\pi} , \tag{24}$$

$$k = \sqrt{\frac{(1+A)(1+B)}{2(A+B)}} , \tag{25}$$

and for $\sqrt{2P} < v_* r_0 - |\kappa_{10} - \kappa_{20}|$

$$\alpha^2 = \frac{A+B}{1+B}, \quad \beta^2 = \frac{\alpha^2}{A}, \quad \gamma = -A\,\mathrm{sgn}(\kappa_{10} - \kappa_{20})$$

$$\omega = \sqrt{(1+A)(1+B)} \frac{v_* K_1 r_0)}{4\pi} ,$$

$$k = \sqrt{\frac{2(A+B)}{(1+A)(1+B)}} .$$

Equations for the center of gravity are given by

$$\frac{1}{2}(x_1 + x_2) = -\frac{\pi r_0}{v_* K_1(r_0)} \frac{d\theta}{dt} - \frac{\kappa_{10} + \kappa_{20}}{2 v_*} , \tag{26}$$

$$\frac{1}{2}\frac{d}{dt}(y_1 + y_2) = \frac{K_1(r_0)}{4\pi} \left[\kappa_{10} - \kappa_{20} + v_* r_o \cos\theta\right] \cos\theta . \tag{27}$$

It must be noted that a vortex-pair ($\kappa_{10} + \kappa_{20} = 0$) propagates in the y-direction without oscillation in the orbit for $\theta_0 (= \theta(t=0)) = n\pi$ (n : integer) and with oscillation for $\theta_0 \neq n\pi$ as is shown in Fig. 1, which has been numerically observed by Makino, Kamimura, and Taniuti[6] based on the Hasegawa-Mima equation. Computations are monitored by keeping P

constant within ten effective figures. In fact the frequency given by Eq. (24) shows the same type of v_*-dependence as those observed in numerical simulations by Makino *et al.*, which is depicted in Fig. 2. Recently Nycander and Isichenko[7] derived the equation for the center of gravity of a vortex-pair from the moment equations of the Hasegawa-Mima equation and obtained the frequency of the trajectory which is also well fitted to the results by Makino *et al.*A non-propagating solution shown in Fig. 1(c) is realized for such initial angles of the symmetry axis of the vortex-pair to the x-axis that the velocity of the vortex-pair given by

$$\begin{aligned}\frac{1}{2}\left\langle\frac{d}{dt}(y_1+y_2)\right\rangle &= \frac{1}{8K(k)}\int_0^{4K(k)} dt\frac{K_1(r_0)}{2\pi}\left[\kappa_{10}-\kappa_{20}+v_* r_0\cos\theta\right]\cos\theta \\ &= \sqrt{2P}\left[1-2\frac{E(k)}{K(k)}\right]\frac{K_1(r_0)}{4\pi} \\ &\equiv c\ . \end{aligned} \tag{28}$$

is zero where $K(k)$ and $E(k)$ are the complete elliptic integral of the first and second kind, respectively. Figure 3 shows the initial angle versus the size of the nonpropagating vortex-pairs for the case of $\kappa_0/v_* = 2.0$. Another example of non-propagating vortex-pair is given in Fig. 4.

Two like-signed vortices ($\kappa_{10} = \kappa_{20}$) are mutually trapped, rotating around the center of graving which is easily seen from Eqs. (26) and (27) (Fig. 5). This mutual trapping leads to coarse-graining of the correlations over directions and may be considered a mechanism behind the fusion of vortices in the sense that a group of point vortices positioned sufficiently near one another acts at large distances as a single vortex with the sum intensity, $\kappa_T \cong \sum_\alpha \kappa_\alpha$. A coalescence of like-signed vortices and a long-lived monopole numerically observed by Horton[4] may be interpreted by this mutual trapping process. The inverse cascade[8] of the energy associated by the conservation of enstrophy is also regarded in the vortex representation as a trapping as a kind of snowballing process.

It is certainly not trivial to determine how many point vortices are necessary to describe

a fluid vortex without losing essential features. A stationary vortex-pair solution[9] of the Hasegawa-Mima equation is characterized by two parameters, the size r_0 and the speed c in terms of which the amplitude is expressed:

$$\phi(r,\theta) = \begin{cases} AK_1\left(\dfrac{\beta r}{r_0}\right)\cos\theta & \text{for } r > r_0 \\ \left[\dfrac{Br}{r_0} + CJ_0\left(\dfrac{\gamma r}{r_0}\right)\right]\cos\theta & \text{for } r < r_0 \end{cases}$$

$$A = \frac{r_0 c}{K_1(\beta)}\ , \quad B = r_0 c\left(1+\frac{\beta^2}{\gamma^2}\right)\ , \quad C = -\left(\frac{\beta}{\gamma^2}\right)\frac{r_0 c}{J_1(\gamma)}\ , \quad \beta = \sqrt{1-\frac{v_*}{c}}$$

and γ is determined by

$$\frac{K_2(\beta)}{\beta K_1(\beta)} + \frac{J_2(\gamma)}{\gamma J_1(\gamma)} = 0\ .$$

The peak amplitude is given in Ref. 9 as well.

On the other hand a point vortex-pair is characterized by the vorticity κ_0 and the size r_0, and its speed is given by Eq. (28). From Eq. (28) we express κ_0 in terms of c and r_0 and compare it with the peak amplitude of the Hasegawa-Mima stationary vortex-pair in Fig. 6, which suggests that point vortex-pairs can be used to study dynamics of the Hasegawa-Mima vortex-pairs, as long as the number of vortices involved is not so large.

IV. Collision Processes of two Vortex-Pairs

Collision processes of two vortex-pairs are shown to recover those observed numerically[6,9,10] for elastic cases with zero (Fig. 7) and non-zero impact parameters (Fig. 8). Since our point vortex model does not take into account effects of interaction with the wake fields, the inelastic collisions with an emission of wake fields observed by McWilliams and Zabusky[10] cannot be described by the vortex field component in Eq. (9) alone. However, the position dependence of the vorticity gives the vortex system studied here a variety of complicated behavior including an exchange scattering and a boomerang scattering (Fig. 9), indicating that our point vortex system is likely to become turbulent when many vortices are involved. However

the potential structure constructed from Eq. (9) is quite orderly as is shown in Fig. 10 which corresponds to Fig. 8(e): mutually trapped vortices behave as a single vortex though dynamics of constituent point vortices are very complicated. Therefore the complication of the dynamics of the point vortices is rather analogous to complicated behaviors of constituent partices in an ordinary gas or fluid dynamics and averaged properties may be of primary importance although the dynamical properties of the point vortex system is academically interesting since the chaotic behavior may be characterized by intermittent structures-clusters of vortices, in which local order is a preferred state because of the short-range interaction force between point vortices. The range of the interaction $\rho_s = c(m_i T_e)^{1/2}/eB$ is given by the parallel electron motion shielding the charge separation in the Euler vortex.

V. A Statistical Theory of Point Vortices and Vortex Diffusion

Here we turn to a statistical system with N point vortices and derive a kinetic equation for vortex diffusion. Introducing a distribution function of vortices of α-species by

$$F_\alpha(\mathbf{r},t) = \sum_j \delta\left(\mathbf{r} - \mathbf{r}_j^{(\alpha)}(t)\right) \ , \tag{29}$$

we immediately obtain the Klimontovich equation[11] for vortices using Eqs. (17) and (18).

$$\frac{\partial}{\partial t}F_\alpha + \mathbf{z} \times \frac{\partial \Phi}{\partial \mathbf{r}} \cdot \frac{\partial}{\partial \mathbf{r}} F_\alpha = 0 \ , \tag{30}$$

$$\Phi(\mathbf{r},t) = \frac{1}{2\pi}\sum_\alpha \int d\mathbf{r}' \kappa_\alpha(\mathbf{r}') K_0(|\mathbf{r}-\mathbf{r}'|) F_\alpha(\mathbf{r}') \ . \tag{31}$$

The averaged distribution function is defined by the average over the ensemble of initial data and the fluctuations:

$$\langle F_\alpha(\mathbf{r},t)\rangle = \int d\mathbf{r}_{10}\cdots d\mathbf{r}_{N0} P_\alpha(\mathbf{r}_{10}\ldots\mathbf{r}_{N0}) F_\alpha(\mathbf{r},t) \ , \tag{32}$$

while the fluctuation part of the distribution function is simply given

$$\tilde{f}_\alpha(\mathbf{r},t) = F_\alpha(\mathbf{r},t) - \langle F_\alpha(\mathbf{r},t)\rangle \tag{33}$$

which includes fluctuations due to the interactions of the vortices and the discreteness of the vortices. Taking the ensemble average of Eq. (30), and subtracting the result from Eq. (30), we get

$$\frac{\partial}{\partial t}\langle F_\alpha\rangle + \mathbf{z}\times\frac{\partial\langle\Phi\rangle}{\partial\mathbf{r}}\cdot\frac{\partial}{\partial\mathbf{r}}\langle F_\alpha\rangle = -\left\langle \mathbf{z}\times\frac{\partial\tilde{\Phi}}{\partial\mathbf{r}}\cdot\frac{\partial\tilde{f}_\alpha}{\partial\mathbf{r}}\right\rangle , \tag{34}$$

and

$$\frac{\partial}{\partial t}\tilde{f}_\alpha + \mathbf{z}\times\frac{\partial}{\partial\mathbf{r}}\left(\langle\Phi\rangle+\tilde{\Phi}\right)\cdot\frac{\partial\tilde{f}_\alpha}{\partial\mathbf{r}} = -\mathbf{z}\times\frac{\tilde{\Phi}}{\partial\mathbf{r}}\cdot\frac{\partial}{\partial\mathbf{r}}\langle F_\alpha\rangle \ . \tag{35}$$

Introducing the Green function

$$\left[\frac{\partial}{\partial t} + \mathbf{z}\times\frac{\partial}{\partial\mathbf{r}}\left(\langle\Phi\rangle+\tilde{\Phi}\right)\cdot\frac{\partial}{\partial\mathbf{r}}\right] G(\mathbf{r},t|\mathbf{r}',t') = \delta(\mathbf{r}-\mathbf{r}')\delta(t-t') \ , \tag{36}$$

Eq. (35) is formally solved in terms of G by

$$\begin{aligned}\tilde{f}_\alpha(\mathbf{r},t) = &\int d\mathbf{r}'dt'G(\mathbf{r},t|\mathbf{r}',t')\delta f(\mathbf{r}',t') \\ &-\int d\mathbf{r}'dt'G(\mathbf{r},t|\mathbf{r}',t')\mathbf{z}\times\frac{\partial\tilde{\Phi}}{\partial\mathbf{r}'}\cdot\frac{\partial}{\partial\mathbf{r}'}\langle F_\alpha\rangle \ ,\end{aligned} \tag{37}$$

where the first term is a contribution of the discreteness. The Green function determined by Eq. (36) has a fluctuating part which is substituted into Eq. (37) to give higher harmonics of the fluctuation. Therefore at the first approximation, we may replace G in Eq. (37) by the average $\langle G\rangle$ to obtain

$$\begin{aligned}\tilde{f}_\alpha(\mathbf{r},t) \simeq &\int d\mathbf{r}'dt'\,\langle G(\mathbf{r},t|r',t')\rangle\,\delta f(\mathbf{r}',t') \\ &-\int d\mathbf{r}'dt'\,\langle G(\mathbf{r},t|\mathbf{r}',t)\rangle\,\mathbf{z}\times\frac{\partial\hat{\Phi}}{\partial\mathbf{r}'}\cdot\frac{\partial}{\partial\mathbf{r}'}\langle F_\alpha\rangle \ ,\end{aligned} \tag{38}$$

The Green function is given by a solution of the characteristic equation of Eq. (36) as

$$G(\mathbf{r},t|r',t') = \delta(\mathbf{r} - \mathbf{r}(t;r',t')) \tag{39}$$

where

$$\begin{aligned}\mathbf{r}(t;r',t') &= \mathbf{r}' + \int_{t'}^{t} dt''\mathbf{z} \times \frac{\partial}{\partial \mathbf{r}}(\langle\Phi(\mathbf{r}(t''),t'')\rangle + \tilde{\Phi}(\mathbf{r}(t''),t'')) \\ &\equiv \mathbf{r}' + \mathbf{V}_E(t-t') + \tilde{\mathbf{r}}(t;r',t') \ . \end{aligned} \tag{40}$$

Therefore the averaged Green function is expressed in terms of cumulants with respect to $\tilde{\mathbf{r}}$:

$$\langle G(\mathbf{r},t|\mathbf{r}',t')\rangle = \sum_k e^{i\mathbf{k}\cdot(\mathbf{r}-\mathbf{r}'-\mathbf{U}_E(t-t'))} e^{\Sigma_n C_n(\mathbf{k}\cdot\tilde{\mathbf{r}})} \ , \tag{41}$$

where $C_n(\mathbf{k}\cdot\tilde{\mathbf{r}})$ denotes the cumulants and the first two terms are given by

$$\begin{aligned} C_1(\mathbf{k}\cdot\tilde{\mathbf{r}}) &= -i\langle\mathbf{k}\cdot\tilde{\mathbf{r}}\rangle \ , \\ C_2(\mathbf{k}\cdot\tilde{\mathbf{r}}) &= -\tfrac{1}{2}\langle(\mathbf{k}\cdot\tilde{\mathbf{r}})^2\rangle - [C_1(\mathbf{k}\cdot\tilde{\mathbf{r}})]^2 \ . \end{aligned}$$

Since our vortex system is characterized by complicated dynamical behaviors of the constituent point vortices, the fluctuatons are likely to deviate from the Gaussian, implying that the higher order cumulants do not vanish. However we may assume, as a model, that the second order cumulant dominates over the others. Then Eq. (41) is approximated by

$$\langle G(\mathbf{r},t|\mathbf{r}',t')\rangle \simeq \sum_{\mathbf{k}} e^{i\mathbf{k}\cdot(\mathbf{r}-r'-\mathbf{U}_E(t-t'))-\mathbf{k}\cdot\mathbf{D}\cdot k(t-t')} \tag{42}$$

where

$$\mathbf{D} = \frac{1}{2}\int_0^\infty d\tau \left\langle \mathbf{z}\times\frac{\partial\tilde{\Phi}(\mathbf{r}(t),t)}{\partial\mathbf{r}} : \mathbf{z}\times\frac{\partial\tilde{\Phi}(\mathbf{r}(t-\tau),t-\tau)}{\partial\mathbf{r}}\right\rangle \ , \tag{43}$$

and we have assumed that the correlation time of the fluctuations is short. Substituting Eqs. (38) and (43) into Eq. (34), we have

$$\frac{\partial}{\partial t}\langle F_\alpha\rangle + \mathbf{z}\times\frac{\partial\langle\Phi\rangle}{\partial\mathbf{r}}\cdot\frac{\partial}{\partial\mathbf{r}}\langle F_\alpha\rangle = \frac{\partial}{\partial\mathbf{r}}\cdot\mathbf{D}\cdot\frac{\partial}{\partial\mathbf{r}}\langle F_\alpha\rangle + \mathbf{A}\cdot\frac{\partial}{\partial\mathbf{r}}\langle F_\alpha\rangle \ , \tag{44}$$

where

$$\mathbf{D} = \sum_{\mathbf{k}} \int \frac{d\omega}{2\pi} \frac{\mathbf{z}\times\mathbf{k} : z\times\mathbf{k}}{-i(\omega - \mathbf{k}\cdot\mathbf{U}_E) + \mathbf{k}\cdot\mathbf{D}\cdot\mathbf{k}} |\tilde{\Phi}(\mathbf{k},\omega)|^2 \ , \tag{45}$$

$$\mathbf{A} = -\frac{i}{2\pi} \sum_{\mathbf{k}} \int \frac{d\omega}{2\pi} \frac{\mathbf{z}\times\mathbf{k}}{\varepsilon(\mathbf{k},\omega)} \left[\kappa_{\alpha 0} \widehat{K}_0(\mathbf{k}) + i v_* \frac{\partial \widehat{K}_0(\mathbf{k})}{\partial k_x} \right]$$

$$\times \frac{1}{(\omega - \mathbf{k}\cdot\mathbf{U}_E)^2 + (\mathbf{k}\cdot\mathbf{D}\cdot\mathbf{k})^2} \ , \tag{46}$$

$$\varepsilon(\omega,\mathbf{k}) = 1 + \frac{i}{2\pi} \sum_{\alpha} \frac{\kappa_{\alpha 0} \widehat{K}_0(\mathbf{k}) + i v_* \frac{\partial \widehat{K}_0}{\partial k_x}}{-i(\omega - \mathbf{k}\cdot\mathbf{U}_E) + \mathbf{k}\cdot\mathbf{D}\cdot\mathbf{k}} \mathbf{k}\cdot z\times\frac{\partial}{\partial \mathbf{r}} \langle F_\alpha(\mathbf{r})\rangle \ , \tag{47}$$

and $\widehat{K}_0$ is the Fourier transform of $K_0(|\mathbf{r}|)$. The second term on the right-hand side of Eq. (44) is a drag term due to the emission of wake fields by the vortices. Since the characteristic frequency of the vortex fluctuation is simply the vortex turn-over time, that is, $\omega \sim \mathbf{k}\cdot\mathbf{U}_E$ which is given by $\epsilon(\omega,\mathbf{k}) = 0$, we may evaluate the vortex diffusion from Eq. (45) as

$$D \sim \frac{1}{D} \sum_{\mathbf{k},\omega} |\tilde{\Phi}(\mathbf{k},\omega)|^2 \sim \left(\sqrt{\sum_{\mathbf{k},\omega} |\tilde{\Phi}(\mathbf{k},\omega)|^2} \right) \ , \tag{48}$$

which by Eq. (31) with $\kappa_0 \leq v_* r_0$ approximately reduces to

$$D \sim N v_* r_0 \ , \tag{49}$$

where r_0 is the average size of the vortices.

From numerical experiments on the vortex collision, Horton[4] found that the cross-section σ for strong inelastic collisions is peaked at the impact parameter comparable to r_0, where $\sigma_{\max} \simeq 2r_0$. Taking the average vortex speed as $c \geq v_*$, he estimated the vortex-vortex collision frequency as

$$\nu \sim n_v c \sigma \sim 2 n_v v_* r_0 \ . \tag{50}$$

This leads to an effective diffusion D of the vortices

$$D = \nu r_0^2 \sim N v_* r_0 \ , \tag{51}$$

which is the same result as that obtained in Eq. (49) by the kinetic theory for point vortices.

VI. Discussion

In this article we have re-derived a point vortex equation introduced by Kono-Yamagata and later Zabusky-McWilliams associated with the Hasegawa-Mima equation and obtained an exact solution for a vortex-pair showing that the dynamical properties of the vortex-pair revealed by numerical simulations based on the Hasegawa-Mima equation are nicely recovered by the point vortex model. Collision processes of two vortex pairs are also examined to show excellent agreement with the results of the numerical simulations, although we have to be careful about differences between the microscopic dynamical state of the point vortex system and the macroscopic dynamical state of the fluid vortex system.. The point vortex system is likely to become chaotic when many vortices are involved. On the other hand the stream function constructed by Eq. (9) from the chaotic dynamics of the point vortices remains regular, being similar to an ordinary gas or fluid dynamics where a flow could be laminar while constituent particles are rondomly agitated. However there can be turbulent states in the macroscopic fluid vortex system. A question is whether the dynamical states of the point vortex system corresponding to the turbulent state of the fluid system is different from that corresponding to the laminar state, and how the turbulent states can be described in terms of the dynamics of the point vortices.

Finally, it is worthwhile to point out that the point vortex system introduced in the present work may be subject to a phase transition to form a vortex lattice, since the interaction force between the point vortices is short range and a local order is likely to be formed. We suggest that further studies of the packing fraction $f_p = n_v \pi r_0^2$ and the vortex-vortex correlation function be used to distinguish between the turbulent states described as vortex gas,[12] a vortex liquid, and a densely packed system approaching a vortex lattice.

Acknowledgment

This work was supported by the U.S. Department of Energy contract #DE-FG05-80ET-53088.

References

1. A. Hasegawa and K. Mima, Phys. Rev. Lett. **39**, 205 (1977); Phys. Fluids **21**, 87 (1978).

2. J. Kono and T. Yamagata, Proc. Oceanogr. Soc. Jpn. **36**, 83 (1977).

3. N. Zabusky and J.C. McWilliams, Phys. Fluids **25**, 2175 (1982).

4. W. Horton, Phys. Fluids B **1**, 524 (1989).

5. A. Hasegawa, C.C. Maclennan, and T. Kodama, Phys. Fluids **22**,2122 (1979).

6. M. Makino, T. Kamimura, and T. Taniuti, J. Phys. Soc. Jpn. **50**, 980 (1981).

7. J. Nycander and M.B. Isichenko, Phys. Fluids B **2**, 2042 (1990).

8. M. Kono and E. Miyashita, Phys. Fluids **31**, 326 (1988).

9. J.D. Meiss and W. Horton, Phys. Fluids **26**, 990 (1983).

10. J.C. McWilliams and N.J. Zabusky, Geophys. Astrophys. Dyn. **19**, 207 (1982).

11. Yu.L. Klimontovich, *The Statistical Theory of Non-Equilibrium Processes in a Plasma* (The M.I.T. Press, 1967).

12. J.D. Meiss and W. Horton, Phys. Rev. Lett. **48**, 1362 (1962); Phys. Fluids **25**, 1838 (1982).

Figure Captions

1. Trajectories of an opposite-signed vortex-pair of $\kappa/v_* = 2.0$ and $r_0 = 0.4$: Solid lines and dotted lines indicate a positive and negative vortex, respectively. Angles between the symmetry axis and x-axis are (a) $\theta_0 = 0$, (b) $\theta_0 = \pi/6$, (c) $\theta_0 = 0.8976$ (d) $\theta_0 = \pi/2$ and (e) $\theta_0 = 2\pi/3$.

2. Frequency of the oscillatory trajectory versus v_* for $\kappa/r_0 = 2.0$ and $c = 0.5$ with initial angles $\theta_0 = n\pi/6$ ($n = 1 \sim 5$ from the bottom)

3. Tilted angle versus the size of the vortex-pair for non-propagating vortex-pairs of $\kappa/v_* = 2.0$.

4. Another type of non-propagating vortex-pair of $\kappa/v_* = 2.0$, $r_0 = 5.0$ and $\theta_0 = 1.6755$.

5. Trajectories of a like-signed vortex-pair: (a) equal vorticity strength $[(\kappa_1, r_1)\ (\kappa_2, r_2) = (20, 2)]$ and (b) strong-weak vorticities $[(\kappa_1, r_1) = (50, 4)$ and $(\kappa_2, r_2) = (20, 2)]$.

6. Size-dependence of the vorticity of the point-vortex propagating in the y direction with $c = 0.5$ and $v_* = 0.4$ and of the peak amplitude of the stationary solution of the Hasegawa-Mima equation with the same speed and the drift velocity.

7. Head-on collision between two opposite-signed vortex-pairs with zero impact parameter.

8. Head-on collision between two opposite-signed vortex-pairs of $\kappa_1/v_* = -1.0$, $\kappa_2/v_* = 1.0$, $\kappa_3/v_* = 2$, and $\kappa_4/v_* = -2.0$ with the initial positions:
   $x_1 = x_{10} + \triangle x_1$, $x_2 = -x_{10} + \triangle x_1$, $x_3 = x_{20} + \triangle x_2$, $x_4 = -x_{20} + \triangle x_2$,
   $x_{10} = 0.25, x_{20} = 0.50$, $y_3 = y_4 = -4.0$ with $(\triangle x_1, \triangle x_2)$: (a) $(0.0, 0.0)$, (b) $(0.15, 0.0)$, (c) $(0.15, 0.15)$, (e) $(0.25, 0.50)$ and $(f)(0.50, 0.50)$.

9. Trajectories of four vortices $\kappa_1/v_* = -\kappa_2/v_* = \kappa_3/v_* = -\kappa_4/v_* = -9.0$ initially located at $x_1 = -x_2 = x_3 = -x_4 = 0.35$, $y_1 = y_2 = -y_3 = -y_4 = 0.2$.

10. Contours of stream function obtained from Eq. (9) using the point vortex trajectories in Fig. 7(e).

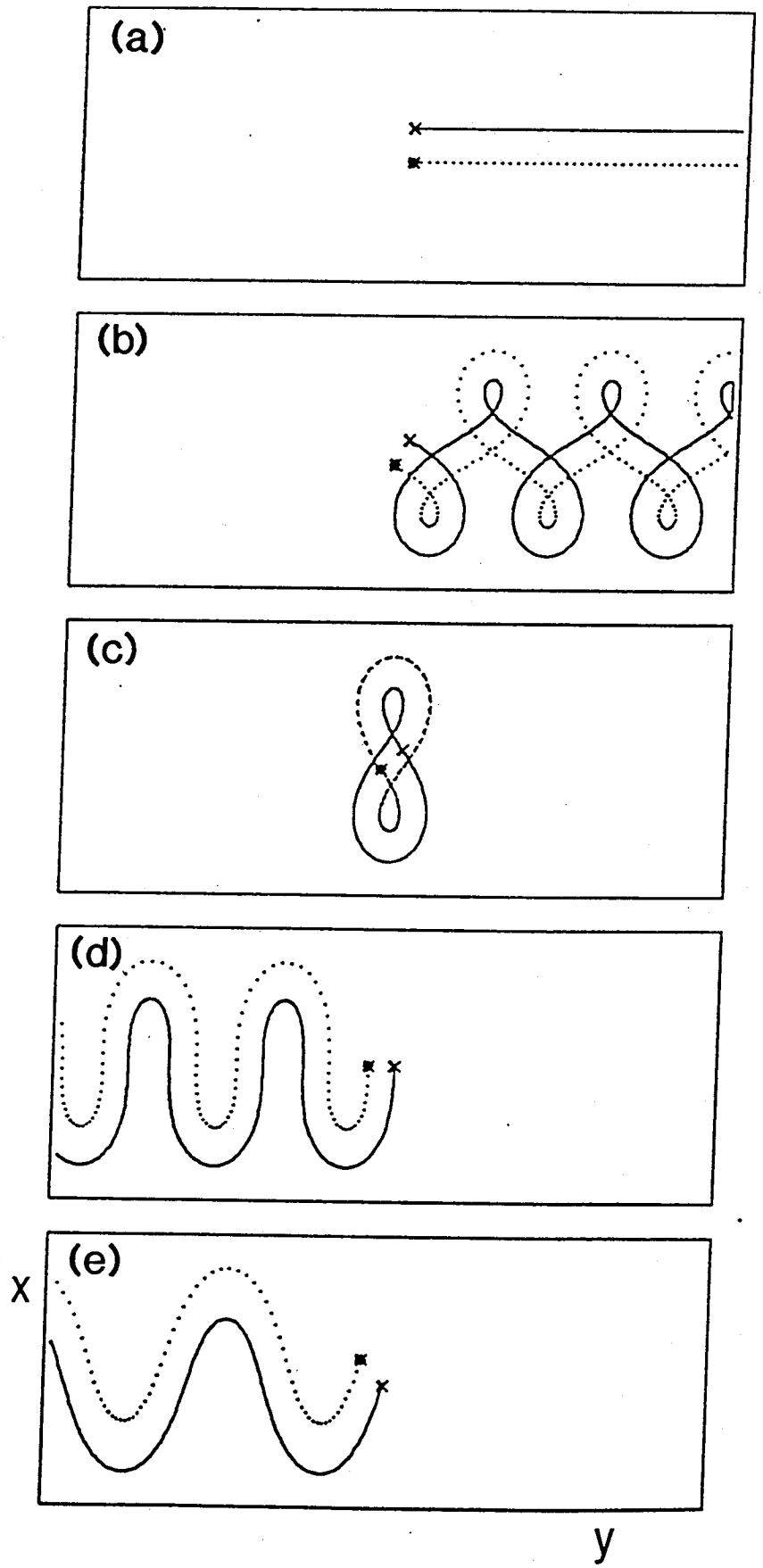

Fig.1

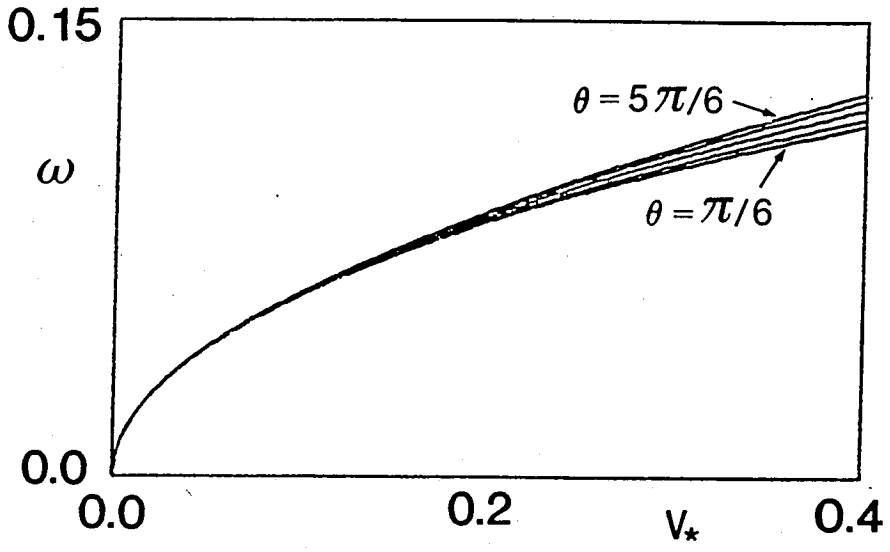

Fig.2

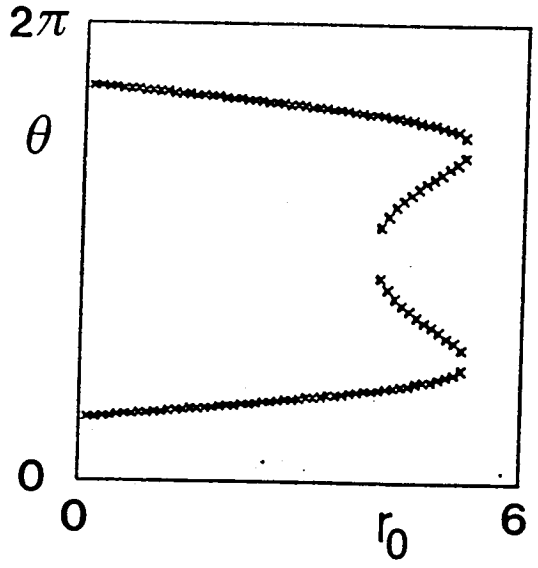

Fig.3

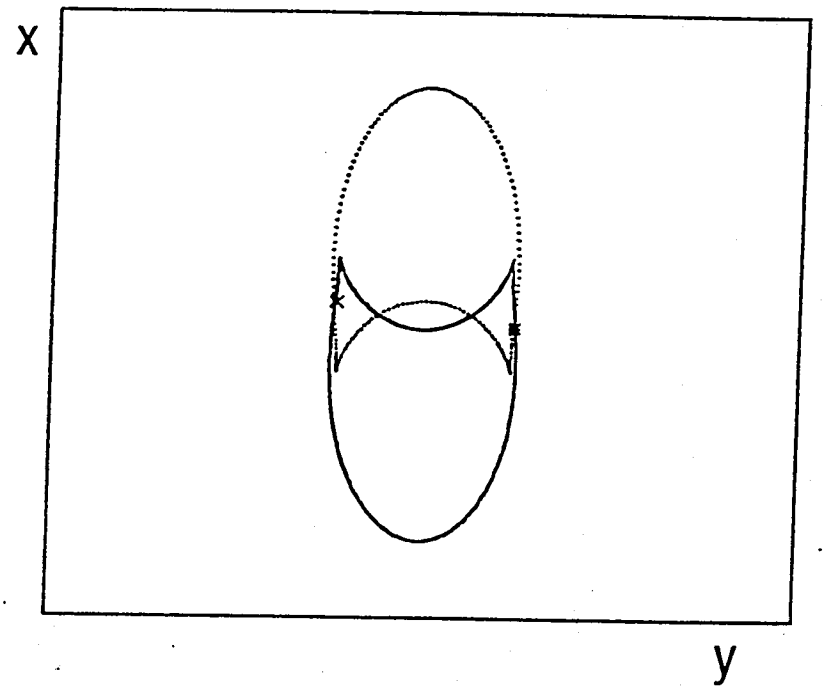

Fig.4

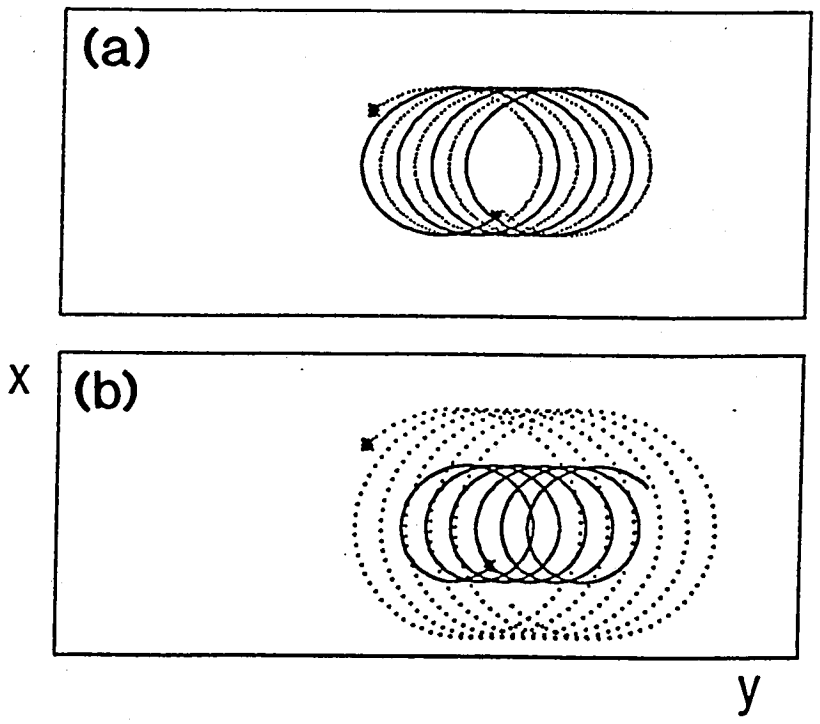

Fig.5

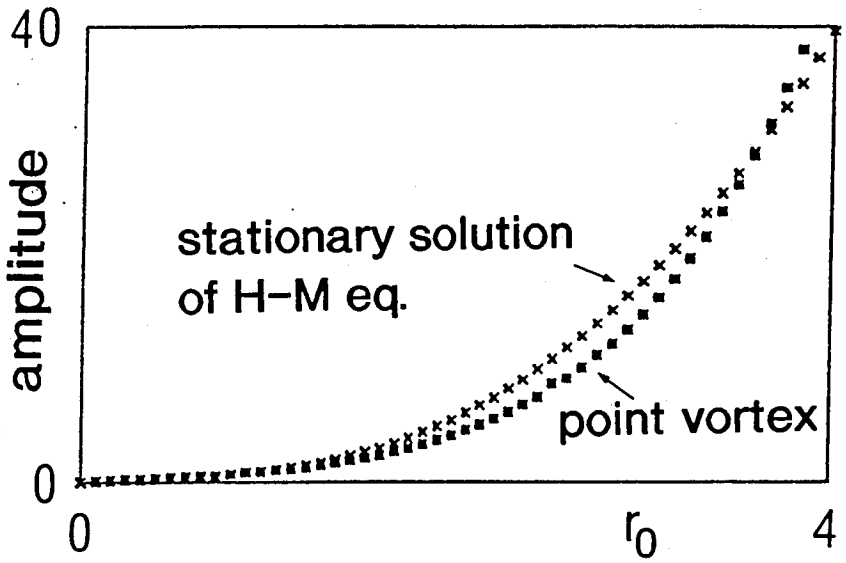
40
amplitude
stationary solution
of H-M eq.
point vortex
0
0
r_0
4

Fig.6

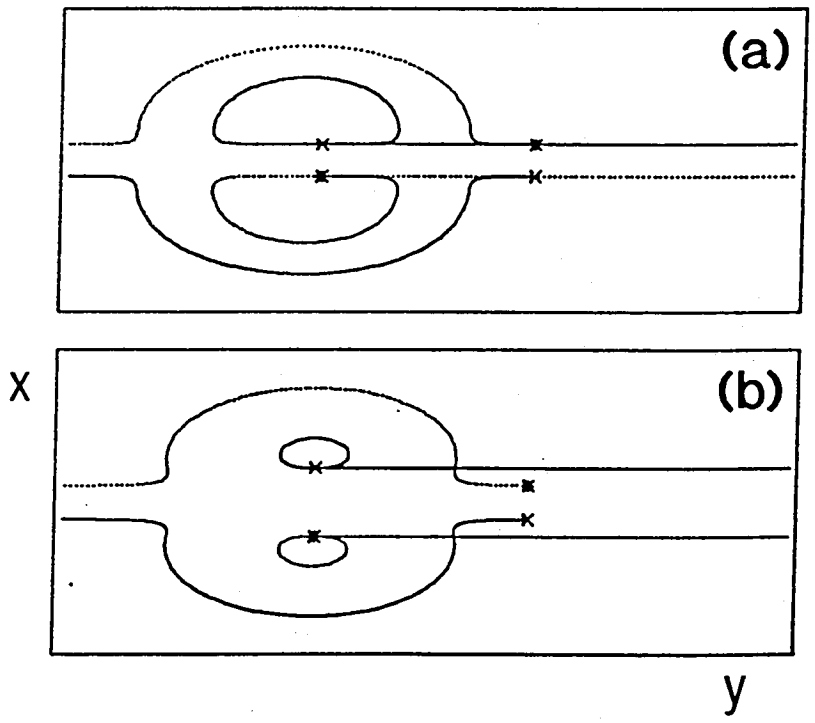
(a)
x
(b)
y

Fig.7

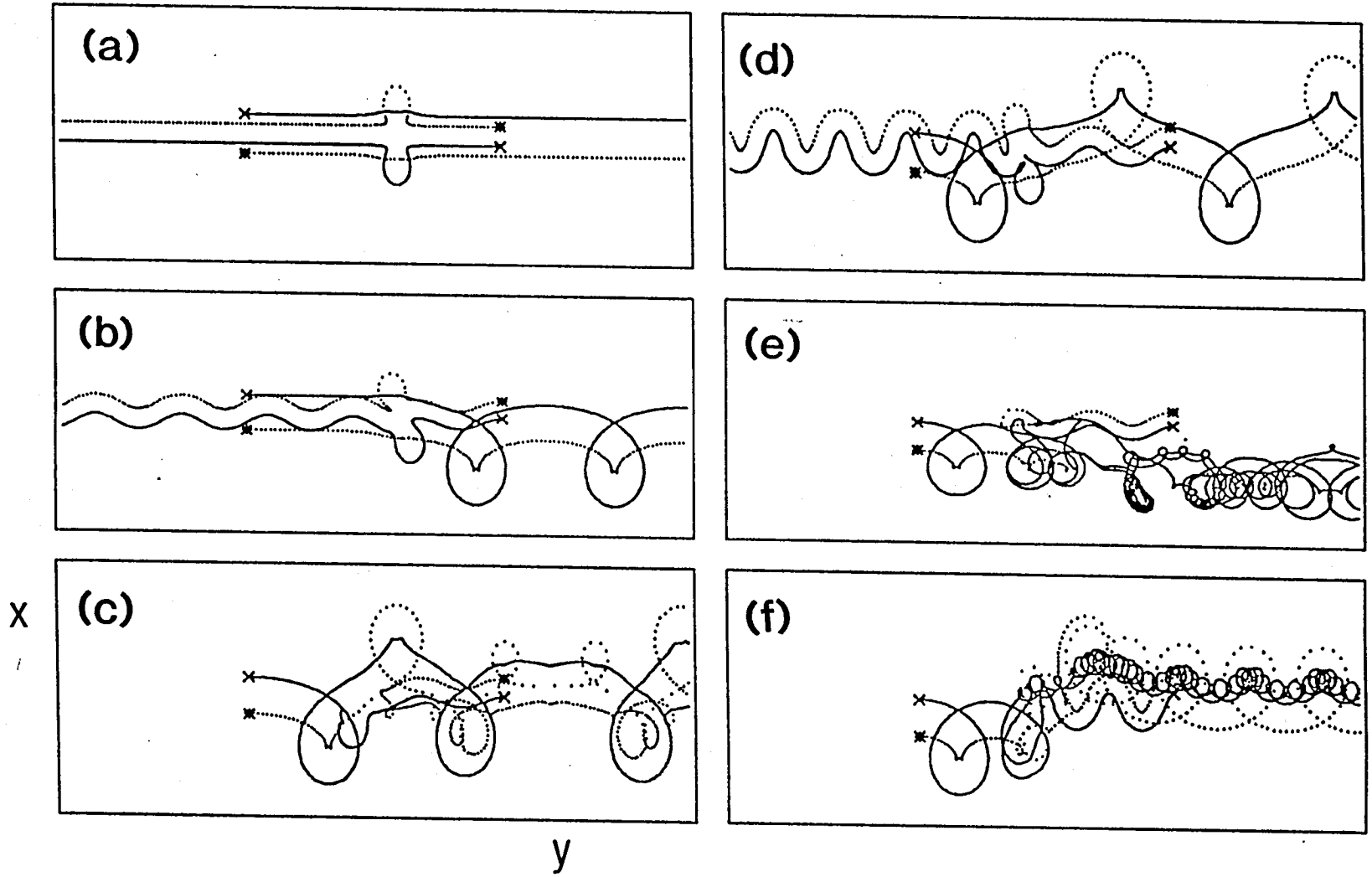

Fig.8

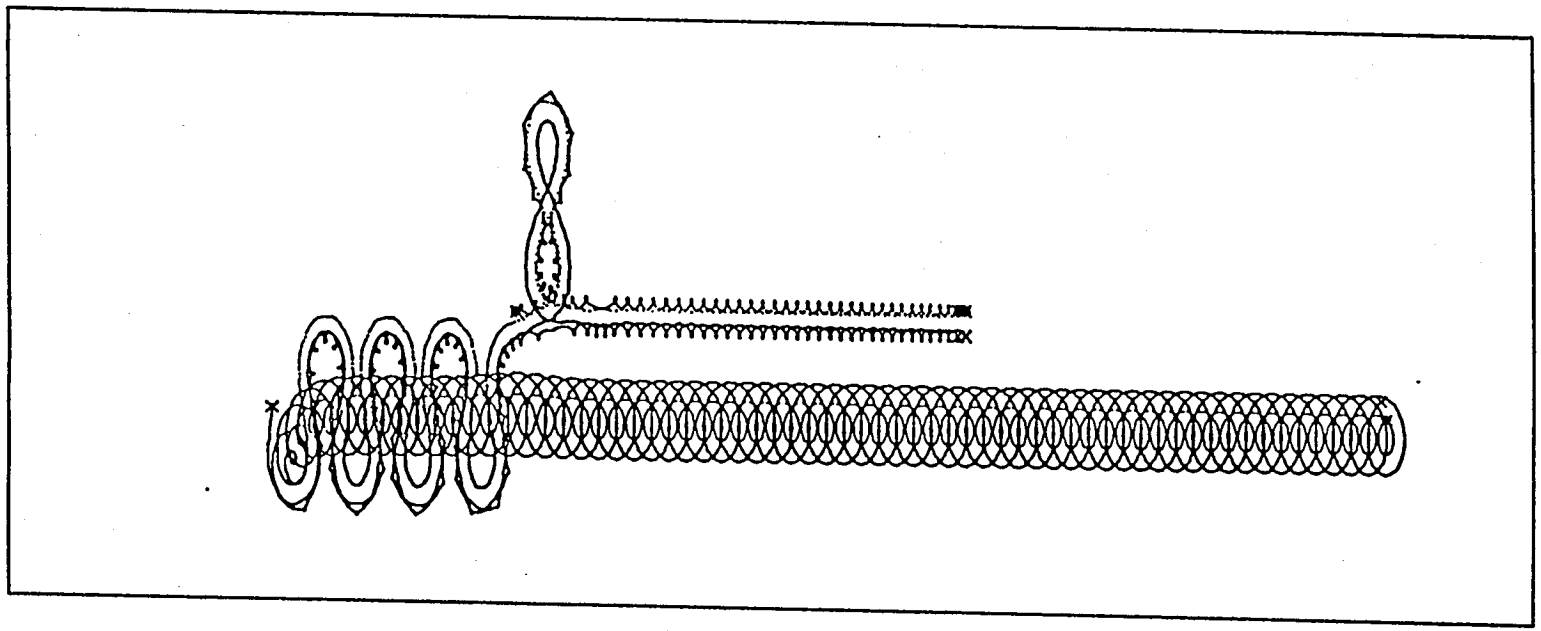

Fig.9

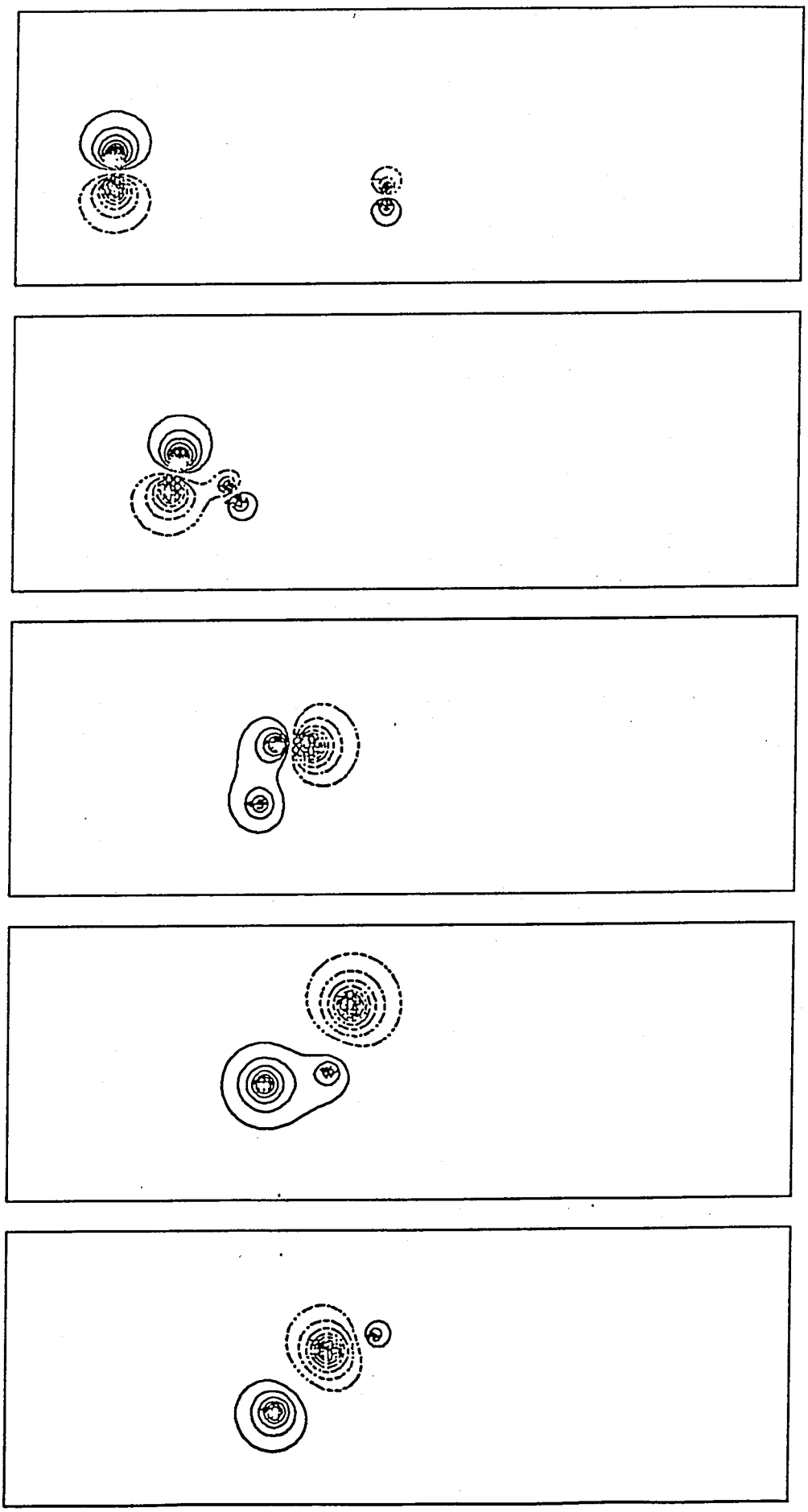

Fig.10

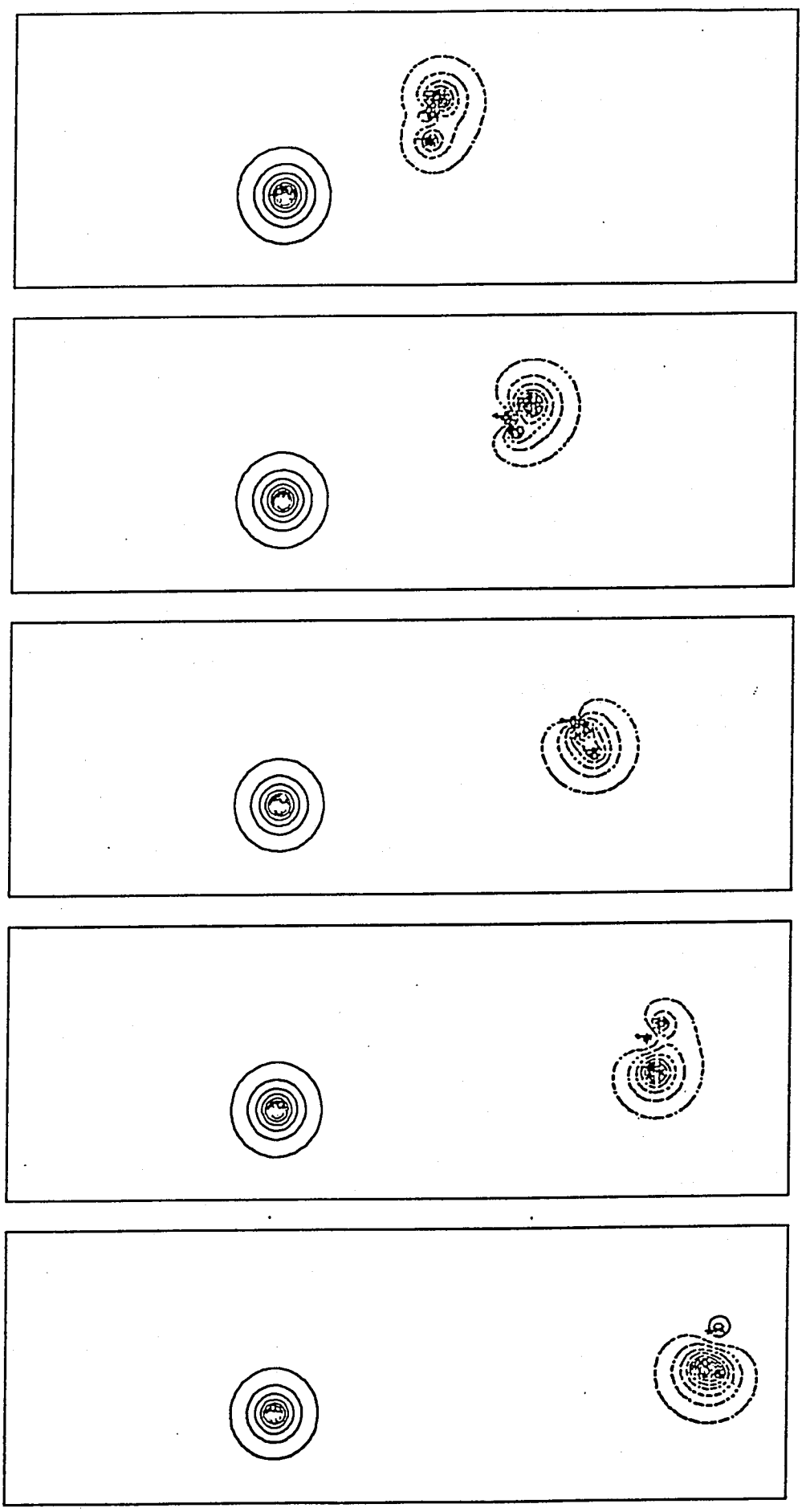

Fig.10 continued